Clinical Ophthalmology

Dovepress
Taylor & Francis Group

Open Access Full Text Article

ORIGINAL RESEARCH

Corneal Alterations in Patients with Osteogenesis Imperfecta: An in vivo Corneal Confocal Microscopy Study

Pietro Mangiantini[1,*], Fabiana Mallone[1,*], Mattia D'Andrea[1], Lorenzo Albanesi[1], Luca Lucchino[1], Luca Celli[2], Mauro Celli[2], Alessandro Lambiase[1], Antonietta Moramarco[1,†]

[1]Department of Sense Organs, Sapienza University, Rome, Italy; [2]Department of Pediatrics, Center for Congenital Osteodystrophy, Sapienza University, Rome, Italy
†Dr Antonietta Moramarco passed away on 24 March 2024
*These authors contributed equally to this work

Correspondence: Alessandro Lambiase, Department of Sense Organs "Sapienza" University of Rome, Viale del Policlinico 155, Rome, 00161, Italy, Tel +390649975305, Fax +390649970364, Email Alessandro.lambiase@uniroma1.it

Purpose: Osteogenesis imperfecta (OI) is a rare hereditary disorder of the connective tissue. Despite recent attention to corneal abnormalities in OI, understanding remains limited. This study aimed to comprehensively evaluate corneal changes in a large sample of OI patients compared to controls using in vivo confocal microscopy (IVCM).

Patients and Methods: Nineteen OI patients (mean age: 34.0 ± 16.00 years; 9 females, 10 males) and 20 healthy controls (mean age: 35.5 ± 12.00; 12 females, 8 males) were included, matched for age and gender. The integrity of corneal cell layers, with a focus on Bowman's layer and sub-epithelial stroma, was evaluated. Additionally, we conducted a quantitative analysis of the corneal sub-basal nerve plexus (CSNP), measuring nerve fiber density (NFD), nerve branch density (NBD), nerve fiber length (NFL), and dendritic cells (DCs) density. Clinical parameters including blue discoloration of the sclera, corneal thickness and sensitivity were also evaluated.

Results: Bowman's layer alterations were observed in 42.11% of OI patients. NFD was significantly reduced in OI patients (27,3 ±6.98 vs controls 37.85±13,74 fiber/mm2; p-value=0.005). NBD and NFL were lower in OI patients but did not reach statistical significance (p=0.650 and p=0.120, respectively). DCs density was higher in OI patients than controls (11,37 ± 12.79 vs 2.09±2,91 cells/mm2; p-value < 0.001). Corneal thickness and sensitivity were significantly reduced in OI patients compared to controls (p<0.001, p=0.001, respectively). OI patients with blue sclera or abnormal Bowman's layer exhibited even lower central corneal thickness (CCT) (p=0.010, p=0.005, respectively).

Conclusion: OI patients demonstrated Bowman's layer abnormalities, neuropathic changes and higher inflammatory cell count. These results suggest potential corneal complications, and hold promise for diagnostic applications and intervention strategies in OI.

Keywords: osteogenesis imperfecta, OI in vivo confocal microscopy, IVCM corneal sub-basal nerve plexus, CSNP corneal nerves, dendritic cells, DCs

Introduction

Osteogenesis imperfecta (OI; MIM#166200, MIM#166210, MIM#259420 and MIM#166220) is a rare hereditary disorder of the connective tissue, with an estimated incidence of ~1:15,000 to 1:20,000 in infants.[1] The disease is characterized by major skeletal manifestations, including bone fracture, deformity, and growth deficiency. Other clinical findings include hearing loss, dentinogenesis imperfecta, hyperlaxity of the ligaments, and cardiovascular diseases.[1] Approximately 90% of cases are caused by dominant mutations in the COL1A1 (MIM#120150) or COL1A2 (MIM#120160) genes, which encode α1(I) and α2(I) chains of type I collagen, respectively.[2]

Type I collagen is a major structural protein in the eye, constituting approximately 90% of the human corneal and scleral extracellular matrix. Additionally, collagen type I is present in the iris, lens, retina, and the Bruch's membrane.[1]

Received: 17 May 2024
Accepted: 17 October 2024
Published: 27 December 2024

An aberrant composition of type I collagen, marked by either structural abnormalities in the protein or quantitative modifications, is a predisposing factor for the development of ocular abnormalities in OI patients.[3–5] Blue discoloration of the sclera is the ocular hallmark in OI, however, other ocular manifestations have been reported and include corneal abnormalities, glaucoma, cataracts, ectopia lentis, retinal detachment, and choroidal neovascularization, among others.[5–7] Specifically, corneal abnormalities have recently gained increased focus in OI, likely prompted by the structural similarities between the cornea and sclera. Notably, the sclera contributes to the stromal layer of the cornea, and both tissues originate from the mesenchyme embryonically. Additionally, both the cornea and sclera are located within the outer fibrous tunic of the eye. Corneal abnormalities reported in OI include corneal thinning and ectasia, reduced corneal hysteresis, keratoconus, congenital absence of the Bowman's layer and corneal rupture due to minor trauma.[5,8]

However, the existing literature on corneal abnormalities in patients with OI relies mostly on case reports or small series, with inconsistencies across studies.[9–11]

Recently, in vivo confocal microscopy (IVCM) has become an increasingly popular noninvasive device to image the cornea at the cellular and microstructural level in healthy as well as diseased corneas. The exploration of the cornea using IVCM in OI is confined to a single documented clinical case which reports an absent or atrophic Bowman's layer along with the absence of sub-Bowman's fibrous structures in two related patients affected by OI.[12]

Therefore, this study was aimed to offer a comprehensive evaluation of corneal morphological changes in a large sample of patients with OI compared to controls using IVCM. Specifically, we conducted a qualitative analysis of all cell layers of the central cornea, focusing specifically on the integrity of the Bowman's layer and sub-epithelial stroma. Additionally, we conducted a quantitative analysis of the corneal sub-basal nerve plexus (CSNP) with measurement of the sub-basal nerve fiber density (NFD), nerve branch density (NBD), nerve fiber length (NFL), and dendritic cells (DCs) density.

Correlations with clinical parameters including blue discoloration of the sclera, central corneal thickness (CCT) and central corneal sensitivity (CCS) were also discussed.

Materials and Methods

This observational, cross-sectional study was conducted at the Sapienza University of Rome, Italy, from November 2022 to January 2023. The current research was approved by the Ethics Committee of Sapienza University of Rome (Prot. N. 0096/2023). The research followed the Tenets of the Declaration of Helsinki, and informed consent was obtained from all subjects of the study and from parents in case of minor age.

All subjects were recruited and evaluated at the Department of Sense Organs, Sapienza University of Rome. Inclusion criteria for patients involved a genetic diagnosis of OI and an age exceeding 14 years. Exclusion criteria were: contact lens wearing, diabetes mellitus, refractive surgery, keratoconus, previous trauma or ocular infection, any coexisting ocular disease that may affect ocular surface.

Healthy subjects, meeting age and sex criteria, were recruited from outpatients of the eye clinic of the "Sapienza" University of Rome, according to the exclusion criteria.

Each subject underwent comprehensive ophthalmological examination, including: detailed medical history collection, Snellen best-corrected visual acuity (BCVA) measurement, anterior segment slit-lamp examination, Goldmann applanation tonometry, mydriatic indirect fundus bio-microscopy. In addition, CCT, CCS, and IVCM of the central cornea were performed in both eyes of all study participants. All assessors were masked to whether patients had OI or not.

CCT

CCT was evaluated using the Sirius Scheimpflug-Placido topographer (CSO, Florence, Italy) which utilizes a single 360-degree rotating Scheimpflug camera combined with a Placido-disk topographer of 22 rings acquiring 25 radial sections of the cornea. A blue light-emitting diode (LED) at a wavelength of 475 nm detects 35,632 points on the anterior cornea and 30,000 points on the posterior cornea. A single measurement was obtained for each subject's eye. Images were captured automatically while subjects fixated on the internal fixation target.

CCS

CCS was assessed using the Cochet-Bonnet aesthesiometer (Luneau Ophthalmologie, Chartres, France). This device employs a fine, retractable, nylon monofilament (0.12 mm diameter) that extends from 5 to 60 mm in length. Adjustable pressure is achievable by modifying the filament's length, with a proportional increase in pressure from 11 to 200 mm/gm as the length decreases.

The procedure started by extending the nylon filament to its maximum length and applying it perpendicularly to the central cornea. When no blink reflex was elicited, the filament was shortened by 1.00 cm. If a positive response was elicited, the thread was moved forward by 0.5 cm. The longest filament length that elicited a positive response was considered the corneal sensitivity threshold, confirmed through two verifications. To account for instrument sensitivity fluctuations related to environmental humidity, all measurements were conducted in a controlled laboratory setting with a humidity range of 50–70% and a temperature maintained between 18–25°C. At the end of the procedure, the filament was sterilized and retracted back into the device to protect from damage.

IVCM

A cornea specific, in vivo, laser confocal microscope (HRT3-RCM; Heidelberg Retina Tomograph 3 with the Rostock Cornea Module, Germany) was used to investigate all cell layers of the central cornea. The HRT3-RCM microscope uses a 670 nm red wavelength diode laser source and scans the imaging field in a raster pattern. A x60 objective water immersion lens with numerical aperture of 0.9 and a working distance of 0.0–3.0 mm was used. This system provides a high-magnification imaging platform of up to 800-fold. The dimensions of each image produced using this lens was 400×400 µm, with a transversal resolution of 2 µm and an optical section thickness of 4 µm. Additionally, this system offers the capability for sequence scans, enabling continuous, dynamic scanning at a user-specified depth. However, it is a contact-based applanation method that might introduce certain artifacts associated with flattening of the corneal surface if not executed correctly.[13–15] In our study, both eyes were anesthetized with a drop of oxybuprocaine hydrochloride 0.4% ophthalmic solution, and polyacrylic acid (Viscotears) served as a coupling agent between the applanation lens cap and the cornea. During the examination every subject was asked to fixate on a distance target aligned to enable the examination on the central cornea. Location of the cornea imaged was within a 2 mm radius of the corneal apex. The full thickness of the central cornea of both eyes was scanned using the device "sequence mode" that enables instantaneous imaging of a single area of the cornea by 100 images performed in 10 seconds. Images were acquired using fixed illumination intensity for all participants.[13] None of the participants reported any visual symptoms or corneal complications following the examination.

IVCM Image Analysis

First of all, a measurement scale was imposed (384 pixel = 400 µm). Image quality was assessed based on sharpness of focus, lack of motion, and good contrast, and blurred images were removed from the analysis sample. There were no post capture image enhancements performed. Two experienced masked IVCM operators performed the confocal examinations and selected the images (L.A. and L.C). Two experienced masked observers, P.M. and F.M. (ophthalmologists), independently carried out qualitative and quantitative evaluations.

Images were acquired from the corneal surface at the corneal epithelial wing cell layer (20 µm of depth), basal epithelium (30 µm of depth), sub-basal nerve plexus (40 µm of depth) Bowman's layer (45 µm of depth), sub-epithelial stroma (150 µm of depth), deep stroma (400 µm of depth), and endothelium (530 µm of depth). The corneal layers were classified as normal based on the criteria outlined in Lagali et al.[16] The integrity of the Bowman's layer and the identification of sub-Bowman's fibrous structures, referred to as K-structures, were evaluated as previously described.[12]

Three of the most representative images of the CSNP were selected for quantitative analysis from the central cornea of each eye from at least 50 good-quality images from each cornea that satisfied the criteria for selection. The CSNP images were considered from the basal epithelial layer and anterior to the Bowman's layer. The typical acquisition depth for these images is between 50 to 70 µm. CSNP images were exported in TIFF format.

Analyses were performed using the semi-automated tracing program NeuronJ (http://www.imagescience.org/meijering/software/neuronj/), a plug-in for ImageJ software (developed by Wayne Rasband, National Institutes of Health, Bethesda, MD; available at http://rsb.info.nih.gov/ij/http://rsb.info.nih.gov/ij/).[12,17,18] ImageJ is a widely used open-

source image processing program. NeuronJ allows for efficient tracing and analysis of neuronal structures within images, enhancing the accuracy and reproducibility of the measurements.[12,17,18]

CSNP parameters analyzed in the study included: (i): corneal nerve fiber density (NFD), the total number of main nerves per millimeter squared (fiber/mm2); nerve branch density (NBD), the total number of branches emanating from the main nerve trunks per millimeter squared (branch/mm2); nerve fiber length (NFL), the total length of all nerve fibers and branches per millimeter squared (mm/mm2). The same image frames were used for quantifying DC density. The count of highly reflective cells with dendriform structures was conducted manually, and the density was derived as the number of cells/mm2. The intraobserver average of results from analyses of the three images from each subject was calculated for each IVCM parameter. If the difference between the two intraobserver averages was less than 15%, an interobserver average for each IVCM parameter was calculated and used for analysis. In case of any inconsistency, a third observer analyzed the images.

One eye was chosen at random for data analysis in each study participant. Descriptive statistical analysis was conducted on all collected data. The Kolmogorov–Smirnov test was performed to assess the normal distribution of continuous variables. Continuous variables were reported as the mean ± standard deviation (SD). For normally distributed variables, an independent Student's *t*-test with Levene's correction was used, and for non-normally distributed variables the Mann–Whitney test was used to compare whether there were significant differences between the groups. Categorical variables were presented as frequencies and percentages, and comparison analysis was conducted using Fisher's exact test. The correlations between age, CCT, CCS, NFD, NBD, NFL, and DCs density were calculated by using the Spearman Rho index or the Pearson analysis, as appropriate. The analysis was conducted using IBM® SPSS® Statistics for Windows®, version 26.0 (IBM Corp., Armonk, NY, USA), and values above the 95% confidence level ($p < 0.05$) were considered statistically significant.

Results

The OI group included 19 patients (9 females and 10 males) aged 14 to 68 years (mean age: 34.0 ± 16.00 years). Among these OI patients, 17 (89,47%) had the COL1A1 mutation, 2 (10,53%) had the COL1A2 mutation, confirmed by molecular genetic testing. All patients were classified as Type I OI according to the Sillence classification.[19] Enrolled healthy controls were 20 (12 females and 8 males) aged between 23 to 65 years (mean age: 35.5 ± 12.00), matched for age and gender (p=0.564 and p=0.527, respectively). Demographic and clinical characteristics of patients and controls are shown in Table 1.

Blue sclera was reported in 11 out of 19 (57,89%) OI patients. The mean CCT in OI patients was 471 ± 55.9 μm, showing a significant difference compared to controls (554 ± 24.5 μm; p<0.001). Notably, a significant reduction in the

Table 1 Demographic and Clinical Characteristics of OI Patients and Controls

	OI (%) (n =19)	Controls (%) (n = 20)	p- value
Age, years (mean ± SD)	34,0 ± 16.00	35,5 ± 12.00	0.564
Gender, n (%)			
Female	9 (47,37)	12 (60,00)	0.527
Male	10 (52,63)	8 (40,00)	
Ethnicity, n (%)			
White	19 (100)	20 (100)	
Black	0 (0,00)	0 (0,00)	1,00
Asian	0 (0,00)	0 (0,00)	
Others	0 (0,00)	0 (0,00)	
Refractive errors, n (%)			
Myopia	5 (26,32)	8 (40,00)	
Astigmatism	7 (36,84)	5 (25,00)	0.606
Hypermetropia	7 (36,84)	7 (35,00)	

(*Continued*)

Table 1 (Continued).

	OI (%) (n =19)	Controls (%) (n = 20)	p- value
Sclera, n (%) **Blue** **Normal**	 11 (57,89) 8 (42,11)	 0 (0,00) 20 (100)	 <0.001
BCVA (Snellen)	20/20	20/20	1,00
Tonometry (mmHg)	13,30 ± 0.67	13,40 ± 0.83	0.238
Central Corneal Thickness (µm)	471 ± 55.90	554 ± 24.50	<0.001
Central Corneal Sensation (cm)	5,58 ± 0.53	6,0 ± 0.00	0.001

Abbreviations: SD, standard deviation; BCVA, best-corrected visual acuity.

mean CCT was observed in OI patients with blue sclera compared to patients without blue sclera (446±59,2 Vs 506 ±25,3 µm; p=0.010). The mean CCS in OI patients was 5.58±0,53 cm, showing a significant difference compared to the control group (6,0±0,0 cm; p=0.001). Results are summarized in Figure 1.

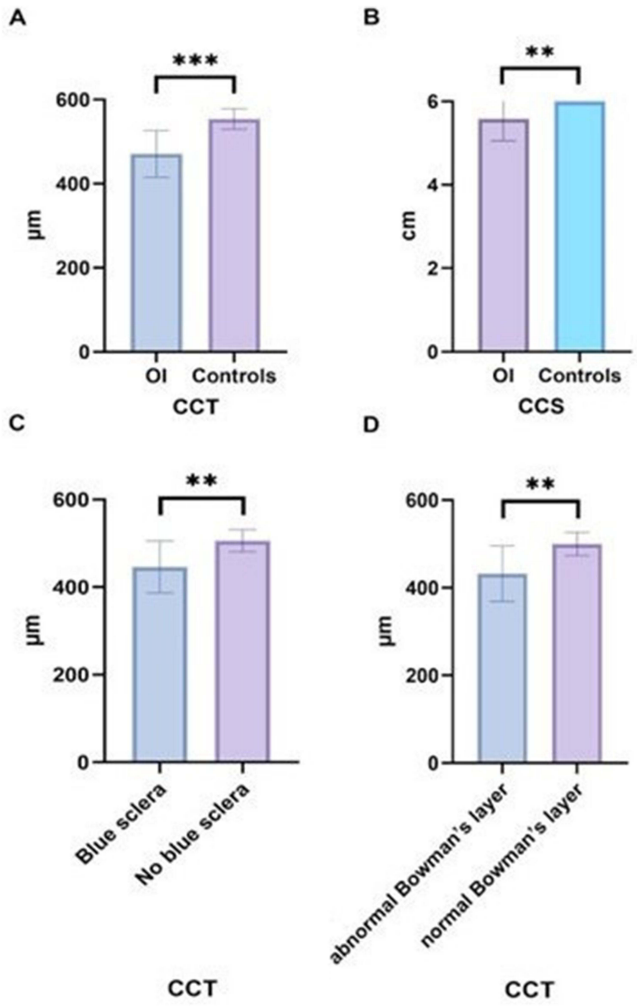

Figure 1 Comparisons of central corneal thickness (CCT) values and central corneal sensitivity (CCS) values between Osteogenesis Imperfecta (OI) patients and controls (**A-B**), comparison of CCT values between OI patients with and without blue sclera (**C**), comparison of CCT values between OI patients with abnormal and normal Bowman's layer (**D**). **: p<0,01. ***: p<0.001.

https://doi.org/10.2147/OPTH.S470183

The epithelial cell layer appeared normal in all patients (Figure 2A and C) and controls (Figure 2B and D) using IVCM. In 8 out of 19 (42,11%) OI patients, the Bowman's layer was absent or barely visible, lacking K-structures between Bowman's layer and sub-epithelial stroma (Figure 3A and C). Among these patients, 6 (75,00%) exhibited blue discoloration of the sclera. In contrast, Bowman's layer was fully intact in all remaining OI patients (11/19, 57.89%; Figure 3B and D) and control subjects (20/20, 100%; refer to Figure 4A and B), with the presence of K-structures beneath the Bowman's layer in the sub-epithelial stroma. The stroma (Figure 5A and B) and endothelial cells (Figure 6A and B) had a normal appearance in both groups.

Interestingly, patients with abnormal Bowman's layer demonstrated a significant lower mean CCT compared to those with normal Bowman's layer (432,38±63,45 Vs 499,82±26,35 µm; p=0.005, refer to Figure 1).

Among nerve parameters, NFD was significantly lower in OI patients compared to controls (27,3 ±6.98 Vs 37.85 ±13,74 fiber/mm2; p-value=0.005). Similarly, NBD and NFL were lower in OI patients compared to controls (26,32 ±13,43 Vs 31.61±21,84 branch/mm^2, 9.97 ±3,06 Vs 12.65 ±4,91 mm/mm^2; respectively), however, results did not reach statistical significance (p=0.650 and p=0.120, respectively).

DCs density was statistically significant higher in OI patients compared to controls (11,37±12,79 Vs 2.09±2,91 cells/mm2; p-value < 0.001). Results are listed in Figure 7.

No significant correlation was observed among the mean CCT, CCS, sub-basal nerve parameters (NFD, NBD, NFL) and DCs density in the OI group (all p values > 0.05).

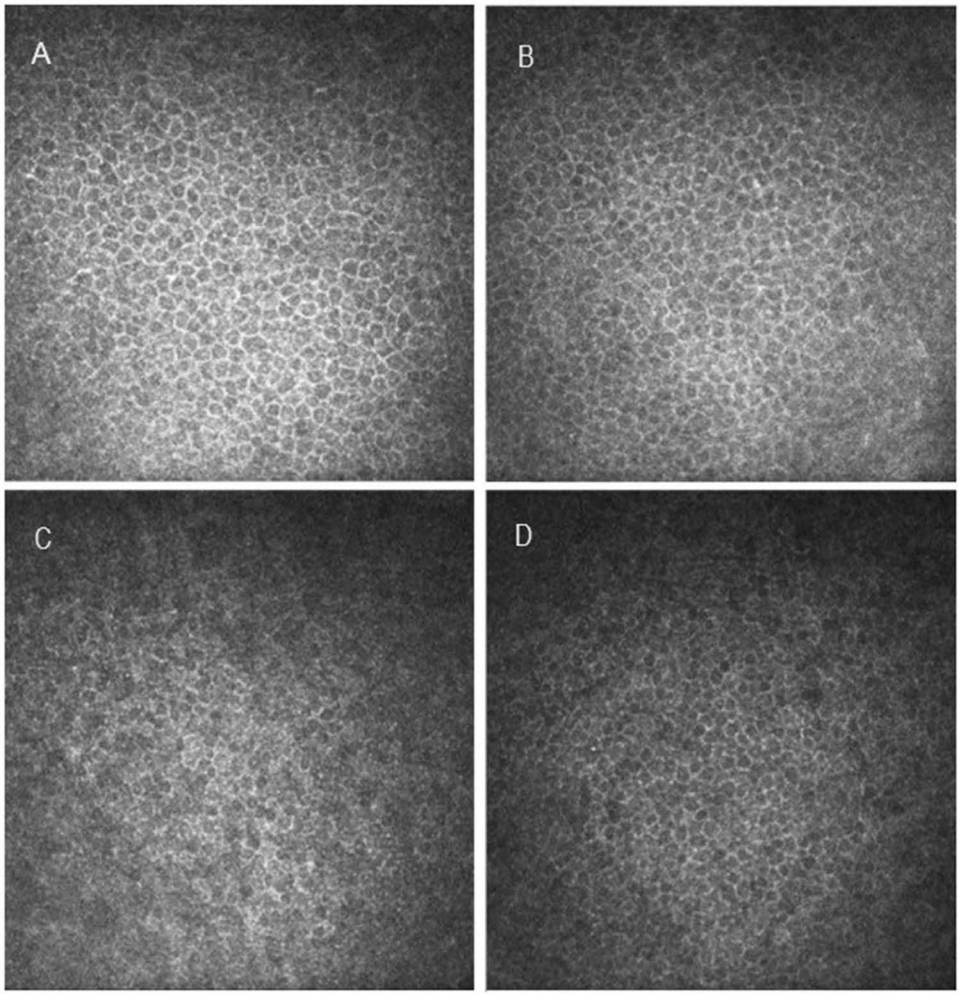

Figure 2 In vivo confocal microscopy (IVCM) images illustrating the normal appearance of the corneal epithelium in both OI patients and controls. The wing cell layer is depicted in panels (**A**) (OI patients) and (**B**) (controls), while the basal cell layer is shown in panels (**C**) (OI patients) and (**D**) (controls).

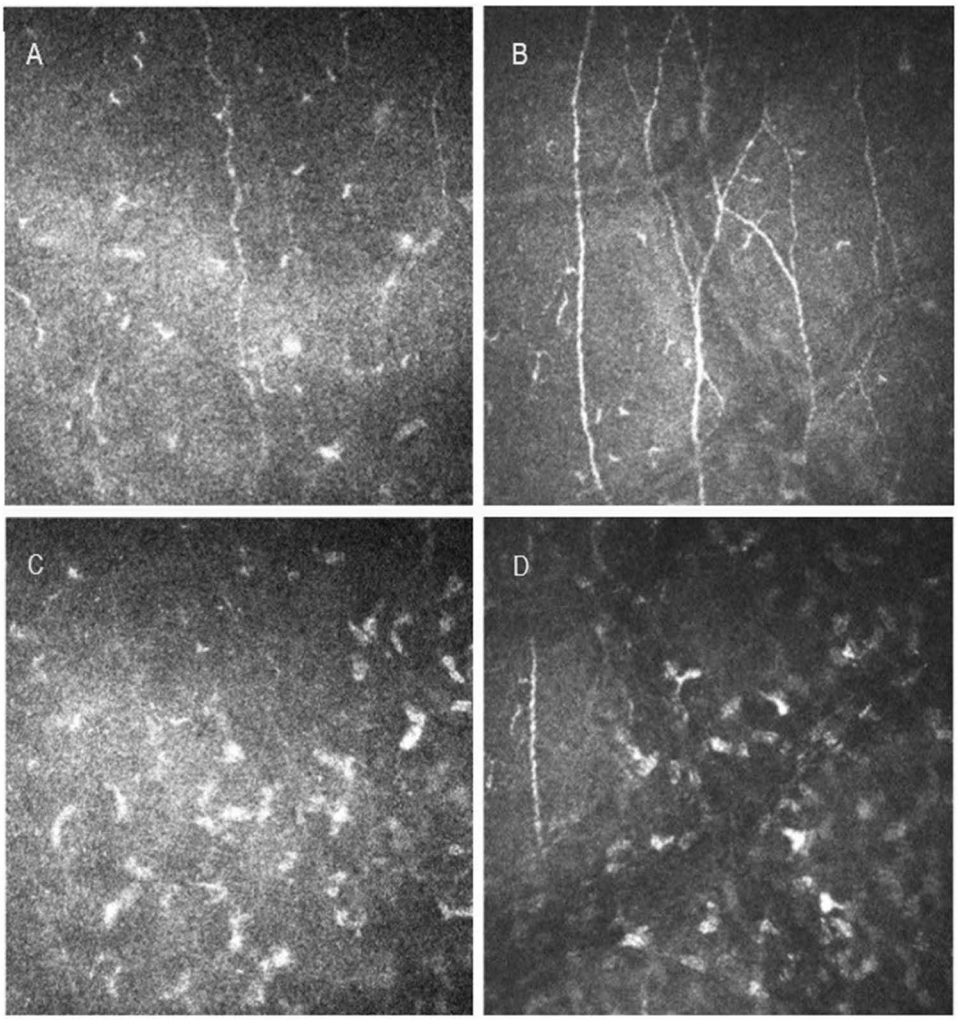

Figure 3 In vivo confocal microscopy (IVCM) images comparing Bowman's layer in OI patients: (**A**) Abnormal Bowman's layer (absent or barely visible), (**B**) Normal Bowman's layer with early visualization of K-structures, (**C**) Absence of K-structures between Bowman's layer and sub-epithelial stroma, (**D**) Normal Bowman's layer with presence of K-structures between Bowman's layer and sub-epithelial stroma.

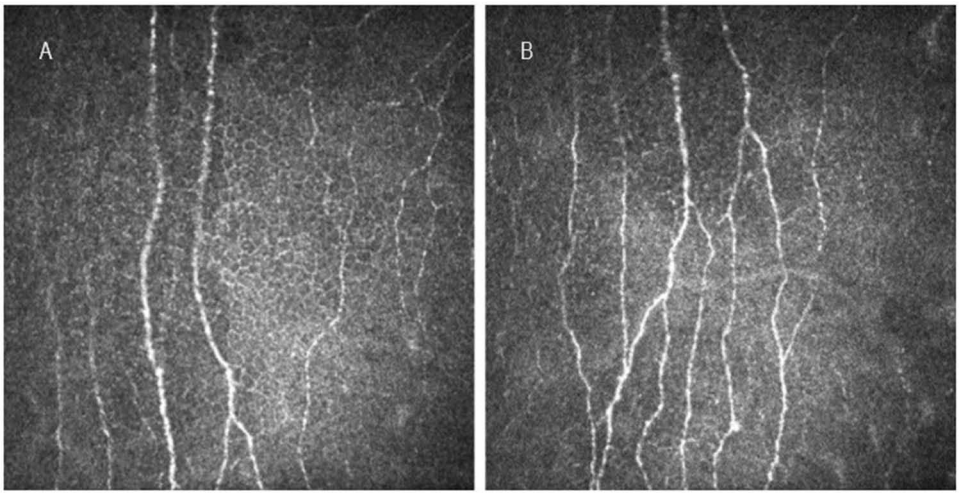

Figure 4 In vivo confocal microscopy (IVCM) images of Bowman's layer with normal appearance (**A**) and presence of K-structures beneath the Bowman's layer in the sub-epithelial stroma (**B**) in a control subject.

https://doi.org/10.2147/OPTH.S470183

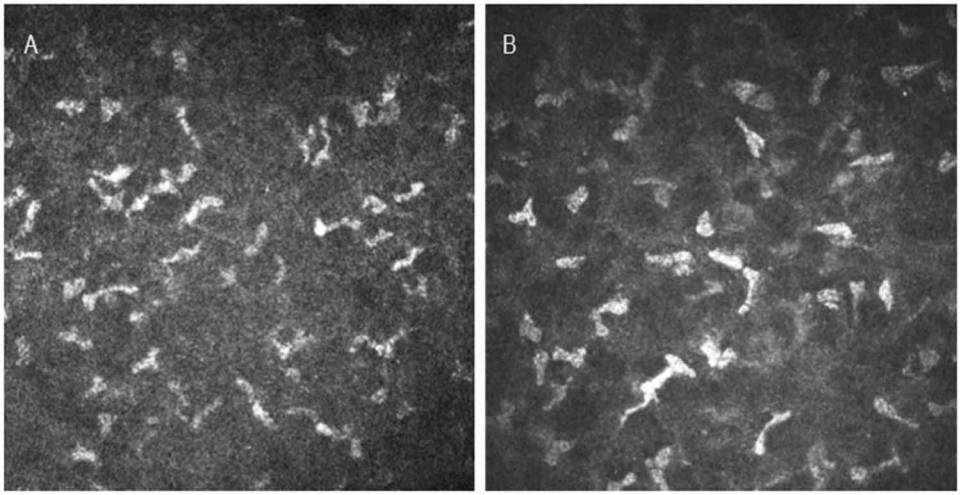

Figure 5 In vivo confocal microscopy (IVCM) images showing the stromal layer with normal appearance in OI patients and controls (**A** and **B**).

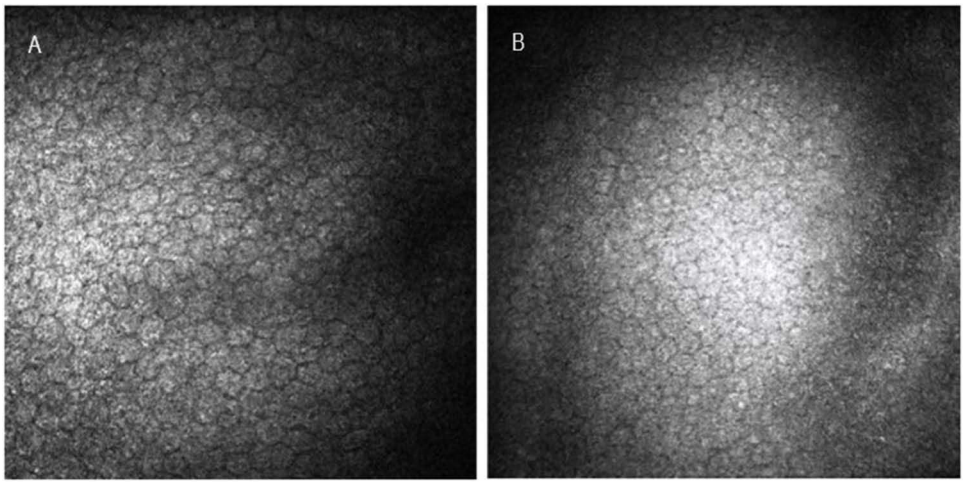

Figure 6 In vivo confocal microscopy (IVCM) images showing endothelial layers with normal appearance in OI patients and controls (**A** and **B**).

Discussion

Our results reported a significant reduction in the mean CCT in OI patients compared to controls (471±55,9 Vs 554 ±24,5 µm; p<0.001). This confirmed previous studies reporting patients with OI to have thinner CCT compared with the control group, with values ranging from 362–571 µm, with 52.9% below 500 µm.4,[9–11] Notably, a significant reduction in the mean CCT was observed in Type-I OI patients with blue sclera compared to Type-I OI patients without blue sclera (446±59,2 Vs 506±25,3 µm; p=0.010) in our sample. These findings are consistent with Everekliogl u et al who demonstrated that Type-I OI eyes with blue sclera had significantly lower CCT readings (446,5±16,3 µm) than type-IV OI eyes without blue sclera (473,6±25,0 µm, p=0.005).[10]

Overall, corneal thinning in OI may arise from defects in the composition or altered distribution of corneal collagen. Histopathology and electron microscopy studies revealed that collagen fibers in the cornea and sclera of individuals with OI were approximately 25% and 50% narrower, respectively, compared to controls. Furthermore, a trace of what was assumed to be the Bowman's layer was scarcely discernible.[20] Recently, an atrophy of Bowman's layer and abnormalities of collagen fibers located between the posterior surface of Bowman's layer and the sub-epithelial stroma[12,21] were reported in two related patients affected by OI using IVCM.[12]

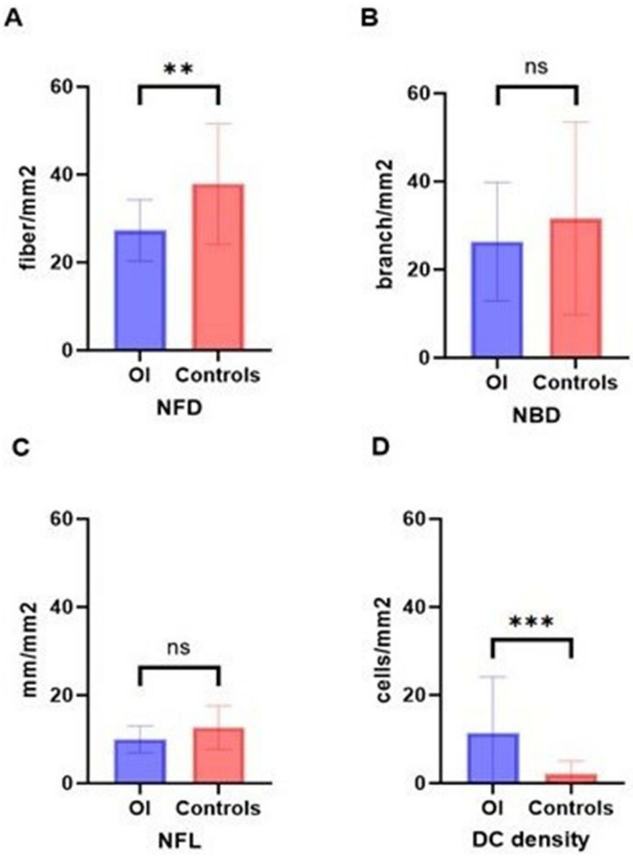

Figure 7 Comparisons of Nerve fiber density (NFD) (**A**), Nerve branch density (NBD) (**B**), Nerve fiber length (NFL) (**C**) and Dendritic cells (DC) density (**D**) values between OI patients and controls. **: p<0,01. ***: p<0.001.
Abbreviation: Ns, non-significant.

In our study, we reported Bowman's layer alterations in 42.11% (8/19) of patients with OI using IVCM. Notably, within this subgroup, six individuals (75,00%) presented with blue discoloration of the sclera.

In these patients, Bowman's layer was hardly detectable, exhibiting a less homogeneous reflectivity compared to OI patients with a normal Bowman's layer. Furthermore, these patients demonstrated the absence of K-structures beneath the Bowman's layer in the sub-epithelial stroma. Conversely, in the remaining OI patients and all control subjects, Bowman's layer remained fully intact and K-structures were present in the sub-epithelial stroma. Interestingly, CCT was significantly lower in OI patients with abnormal Bowman's layer compared to OI patients with a normal Bowman's layer (p=0.005). The appearance of the other corneal layers was found to be normal in OI patients and controls in our study.

Our findings, which report Bowman's layer abnormalities and complete loss of sub-Bowman's K-structures in a significant proportion of OI patients, align with the observations by Kobayashi et al.[12] Moreover, we observed a significant reduction in corneal thickness among OI patients exhibiting abnormal Bowman's layer. This confirms the hypothesis of an association between corneal stromal thinning and an altered Bowman's layer previously hypothesized by the same Authors.[12] These results may suggest corneal complications and hold promise for diagnostic applications in OI. Additionally, we conducted a quantitative assessment of the CSNP by evaluating NFD, NBD, NFL and DCs density. Among nerve parameters, NFD was significantly reduced in OI patients compared to controls (27,3±6.98 Vs 37.85±13,74 fiber/mm2; p-value=0.005). Similarly, NBD and NFL were lower in OI patients compared to controls, however, results did not reach statistical significance (p=0.650 and p=0.120, respectively).

These findings substantiate the existence of neuropathic changes in OI, which aligns with earlier reports of neurological manifestations in individuals with this condition.[22] DCs density was statistically significantly higher in OI patients compared to controls (11,37±12,79 Vs 2.09±2,91 cells/mm2; p-value < 0.001). DCs are immune cells tasked

with internalizing, processing, and exposing antigens on their surface, thereby triggering the immune response by T and B lymphocytes. Recent studies have shown the presence of DCs as immature cells residing in the basal layer of the corneal epithelium and in the anterior stroma.[23]

Our findings, which indicate an elevation in DCs count in OI, support the hypothesis implicating inflammation as a primary factor in the pathogenesis of this disease. Accordingly, previous research reported the activation of inflammatory pathways in OI driven by structural abnormalities and recurrent fractures.[24,25] Specifically, Salter et al observed that elevated bone turnover in OI may trigger inflammation, leading to the release of pro-inflammatory cytokines, such as transforming growth factor-ß (TGFß).[24]

Furthermore, our results, indicating lower NFD alongside a higher DCs count, support a potential interconnection between nervous and immune pathways in OI.[26,27]

Similarly, a significant impairment of innervation in the sub-basal nerves concurrent with an elevated corneal DCs density has been reported in other inflammatory conditions affecting the CSNP such as keratoconus, dry eye disease, and diabetes.[28] Notably, a link between OI and keratoconus has been suggested.[29–31] Also, the mean CCS in OI patients was 5.58±0,53 cm, showing a significant difference compared to the control group (6,0±0,0 cm; p=0.001). However, CCS showed no significant correlation with the density of sub-basal nerve fibers as assessed by IVCM. This could be ascribed to the subclinical nature of corneal neuropathic damage in OI. In accordance, Patel et al discovered no correlation between corneal aesthesiometry and sub-basal nerve density in healthy subjects.[32]

Additionally, Hamrah et al demonstrated that functional alterations in the CSNP begin to manifest only when densitometric data undergo substantial deterioration.[33]

As a limit to the present study, the cross-sectional design prevents us from assessing the potential progression over time of the abnormalities identified by IVCM and clinically. Moreover, keratometry indices were not included, limiting the topographical assessment to central pachymetry in this study.

In conclusion, the investigation of corneal abnormalities in OI has recently gained attention, likely prompted by the structural similarities between the cornea and the sclera. For the first time, IVCM was used to analyze the microstructural features of the cornea and its sub-basal nerve plexus in a large sample of OI patients.

Our study presents significant findings regarding corneal changes in patients with OI. We observed abnormalities in Bowman's layer and complete loss of sub-Bowman's K-structures in a considerable proportion of OI patients, which adds valuable insights to the existing knowledge. Additionally, our study revealed a reduction in corneal innervation in OI compared to controls, indicating the presence of neuropathic changes in the condition. Moreover, an elevation in inflammatory cell count was observed in OI patients, which confirmed inflammation as a primary factor in the disease pathogenesis. Furthermore, our observation of a lower corneal innervation and a higher inflammatory cell count in the sub-basal nerve plexus suggests a possible interplay between nervous and immune pathways in OI.

Based on these findings, corneal morphometric parameters could serve as a useful tool for early diagnosis, assessing disease progression, guiding therapeutic approaches and monitoring response to therapies in OI.

However, confirming these findings requires additional prospective, longitudinal studies with larger sample sizes.

We believe that these results offer promising prospects for advancing diagnostic applications and intervention strategies for individuals affected by OI.

Data Sharing Statement

The data used to support the findings of this study are not openly available due to reasons of sensitivity and are available from the corresponding author upon reasonable request. Data are located in controlled access data storage at Sapienza University.

Ethical Approval

All procedures performed in studies involving human participants were in accordance with the ethical standards of the institutional research committee of Sapienza University of Rome (Prot. N. 0096/2023) and with the 1964 helsinki Declaration and its later amendments or comparable ethical standards.

Informed Consent

Informed consent was obtained from all individual participants included in the study.

Acknowledgments

Dr Antonietta Moramarco passed away on 24 March 2024. She conceived the study, coordinated the writing of the article, and critically evaluated the accuracy and integrity of the work.

Author Contributions

All authors made a significant contribution to the work reported, weather that is in the conception, study design, execution, acquisition of data, analysis and interpretation, or in all these areas; took part in drafting, revising or critically receiving the article; gave final approval of the version to be published; have agreed on the journal to which the article has been submitted; and agree to be accountable for all aspect of the work.

Funding

This work was supported by the No financial support has been requested for the study.

Disclosure

All authors certify that they have no financial or proprietary interest in the subject matter or materials discussed in this manuscript. The authors declare that they do not have any conflicts or potential conflicts of interest.

References

1. Forlino A, Marini JC. Osteogenesis imperfecta. *Lancet*. 2016;387(10028):1657–1671. doi:10.1016/S0140-6736(15)00728-X
2. Van Dijk FS, Sillence DO. Osteogenesis imperfecta: clinical diagnosis, nomenclature and severity assessment. *Am J Med Genet A*. 2014;164A:1470–1481. doi:10.1002/ajmg.a.36545
3. Steiner R, Basel D. COL1A1/2 osteogenesis imperfecta. 2021.
4. Magalhaes OA, Rohenkohl HC, De Souza LT, Schuler-Faccini L, Félix TM. Collagen I defect corneal profiles in osteogenesis imperfecta. *Cornea*. 2018;37:1561–1565. doi:10.1097/ICO.0000000000001764
5. Treurniet S, Burger P, Ghyczy EAE, et al. Ocular characteristics and complications in patients with osteogenesis imperfecta: a systematic review. *Acta Ophthalmol*. 2022;100:e16–e28. doi:10.1111/aos.14882
6. Keleş A, Doğuizi S, Şahin NM, Koç M, Aycan Z. Anterior segment findings in patients with osteogenesis imperfecta: a case-control study. *Cornea*. 2020;39:935–939. doi:10.1097/ICO.0000000000002345
7. Wallace D, Chau F, Santiago-Turla C. Osteogenesis imperfecta and primary open angle glaucoma: genotypic analysis of a new phenotypic association. *Mol Vision*. 2014;20:1174–1181.
8. Correia Barão R, Santos M, Marques RE, Quintas AM, Guerra P. Keratoconus tomographic indices in osteogenesis imperfecta. *Graefes Arch Clin Exp Ophthalmol*. 2023;261:2585–2592. doi:10.1007/s00417-023-06059-4
9. Pedersen U, Bramsen T. Central corneal thickness in osteogenesis imperfecta and otosclerosis. *ORL J Otorhinolaryngol Relat Spec*. 1984;46:38–41. doi:10.1159/000275682
10. Evereklioglu C, Madenci E, Bayazıt YA, et al. Central corneal thickness is lower in osteogenesis imperfecta and negatively correlates with the presence of blue sclera. *Ophthalmic Physiol Opt*. 2002;22(6):511–515. doi:10.1046/j.1475-1313.2002.00062.x
11. Dimasi D, Chen JY, Hewitt AW, et al. Novel quantitative trait loci for central corneal thickness identified by candidate gene analysis of osteogenesis imperfecta genes. *Hum Genet*. 2010;127(1):33–44. doi:10.1007/s00439-009-0729-3
12. Kobayashi A, Higashide T, Yokogawa H, et al. In vivo laser confocal microscopy findings of a cornea with osteogenesis imperfecta. *Clin Ophthalmol*. 2014;8:429–433. doi:10.2147/OPTH.S58087
13. Patel DV, Ku JYF, Johnson R, McGhee CNJ. Laser scanning in vivo confocal microscopy and quantitative aesthesiometry reveal decreased corneal innervation and sensation in keratoconus. *Eye*. 2009;23(3):586–592. doi:10.1038/eye.2008.52
14. Pahuja NK, Shetty R, Nuijts RMMA, et al. An in vivo confocal microscopic study of corneal nerve morphology in unilateral keratoconus. *BioMed Res Int*. 2016;2016:1–5. doi:10.1155/2016/5067853
15. Guthoff RF, Baudouin C, Stave J. Confocal laser scanning in vivo microscopy. *Atlas Confocal Laser Scanning in-vivo Microsc Ophthalmol*. 2006;31–148. doi:10.1007/3-540-32707-X_5
16. Lagali N, Bourghardt B, Germundsson J, et al. Laser-scanning in vivo confocal microscopy of the cornea: imaging and analysis methods for preclinical and clinical applications. *Confocal Laser Microsc - Princ Appl Med Biol Food Sci*. 2013. doi:10.5772/55216
17. Meijering E, Jacob M, Sarria J-CF, et al.Design and validation of a tool for neurite tracing and analysis in fluorescence microscopy images. *Cytometry A*. 2004;(2):167–176. doi:10.1002/cyto.a.20022
18. Meijering E. Neuron tracing in perspective. *Cytometry A*. 2010;77(7):693–704. doi:10.1002/cyto.a.20895
19. Sillence DO, Senn A, Danks DM. Genetic heterogeneity in osteogenesis imperfecta. *J Med Genet*. 1979;16:101–116. doi:10.1136/jmg.16.2.101
20. Sillence DO, Barlow KK, Cole WG. Osteogenesis imperfecta type III. Delineation of the phenotype with reference to genetic heterogeneity. *Am J Med Genet*. 1986;23:821–832. doi:10.1002/ajmg.1320230309

21. Yokogawa H, Kobayashi A, Sugiyama K. Mapping of normal corneal K-structures by in vivo laser confocal microscopy. *Cornea*. 2008;27:879–883. doi:10.1097/ICO.0b013e318170aed0
22. Charnas LR, Marini JC. Neurologic profile in osteogenesis imperfecta. *Connect Tissue Res*. 1995;31:s23–s26. doi:10.3109/03008209509116828
23. Hamrah P, Dana MR. Corneal antigen-presenting cells. *Chem Immunol Allergy*. 2007;92:58–70.
24. Salter L, Offiah AC, Bishop N. Elevated platelet counts in a cohort of children with moderate-severe osteogenesis imperfecta suggest that inflammation is present. *Arch Dis Child*. 2018;103:767–771. doi:10.1136/archdischild-2017-313859
25. Damian LO, Miclea D, Vulturar R, Crăciun A. Osteogenesis imperfecta and rheumatoid arthritis: connective issues. *Osteoporos Int*. 2022;33:2237–2239. doi:10.1007/s00198-022-06530-8
26. Mandathara PS, Stapleton FJ, Kokkinakis J, Willcox MDP. A pilot study on corneal Langerhans cells in keratoconus. *Cont Lens Anterior Eye*. 2018;41:219–223. doi:10.1016/j.clae.2017.10.005
27. Tavakoli M, Boulton AJM, Efron N, Malik RA. Increased Langerhan cell density and corneal nerve damage in diabetic patients: role of immune mechanisms in human diabetic neuropathy. *Cont Lens Anterior Eye*. 2011;34:7–11. doi:10.1016/j.clae.2010.08.007
28. Abicca I, Giannini D, Gilardi M, et al. A novel algorithm for the evaluation of corneal nerve beadings by in vivo confocal microscopy in patients with type 1 diabetes mellitus. *Front Med*. 2022;9. doi:10.3389/fmed.2022.897259
29. Cruzat A, Witkin D, Baniasadi N, et al. Inflammation and the nervous system: the connection in the cornea in patients with infectious keratitis. *Invest Ophthalmol Vis Sci*. 2011;52:5136–5143. doi:10.1167/iovs.10-7048
30. Tuisku IS, Konttinen YT, Konttinen LM, Tervo TM. Alterations in corneal sensitivity and nerve morphology in patients with primary Sjögren's syndrome. *Exp Eye Res*. 2008;86:879–885. doi:10.1016/j.exer.2008.03.002
31. Shaheen BS, Bakir M, Jain S. Corneal nerves in health and disease. *Surv Ophthalmol*. 2014;59:263–285. doi:10.1016/j.survophthal.2013.09.002
32. Patel DV, Tavakoli M, Craig JP, Efron N, McGhee CNJ. Corneal sensitivity and slit scanning in vivo confocal microscopy of the subbasal nerve plexus of the normal central and peripheral human cornea. *Cornea*. 2009;28:735–740. doi:10.1097/ICO.0b013e318193e0e3
33. Hamrah P, Cruzat A, Dastjerdi MH, et al. Corneal sensation and subbasal nerve alterations in patients with herpes simplex keratitis: an in vivo confocal microscopy study. *Ophthalmology*. 2010;117:1930–1936. doi:10.1016/j.ophtha.2010.07.010